

EVOLUTION OF A HIGH REYNOLDS NUMBER ADVERSE-PRESSURE GRADIENT TURBULENT BOUNDARY LAYER FROM A CANONICAL UPSTREAM CONDITION

Mitchell Lozier¹, Ahmad Zarei¹, Ivan Marusic¹ and Rahul Deshpande¹

¹Department of Mechanical Engineering, The University of Melbourne, Victoria 3010, Australia

ABSTRACT

An experimental investigation of the streamwise evolution of an adverse-pressure gradient (APG) turbulent boundary layer (TBL) on a smooth wall, developing from a ‘canonical’ upstream condition (*i.e.* a high Reynolds number zero-pressure gradient (ZPG) TBL), will be presented. Results will be shown for multiple measurement stations along the extensive fetch of the large Melbourne wind tunnel, the test section of which has been modified to investigate this unique APG TBL at high Reynolds numbers, for the first time. Oil-film interferometry (OFI) measurements were conducted at each station, to independently measure the skin friction and estimate the friction velocity. Hot-wire measurements were also conducted to confirm the canonical upstream condition, and then investigate the subsequent development of the moderately-strong APG TBL in the downstream section.

INTRODUCTION

While the Reynolds number is the key parameter influencing the flow physics for incompressible ZPG smooth-wall (*i.e.* canonical) TBLs, wall-bounded flows found in nature almost always have non-canonical complexities, introducing a dependence on additional flow parameters (Clauser, 1954). In the present study, we limit our focus to smooth-wall TBLs exposed to an APG, which are commonly encountered over airplane wings or in diffusers, for example. In addition to the friction Reynolds number (Re_τ), previous studies have found that the APG strength and the upstream pressure gradient history also influence TBL characteristics (Bobke *et al.*, 2017). Here, we define $Re_\tau = \delta_{99}U_\tau/\nu$, where δ_{99} is the TBL thickness, U_τ is the friction velocity and ν is the kinematic viscosity. The strength of the pressure gradient is typically quantified by the Clauser pressure gradient parameter, $\beta(x) = (\delta^*/\rho U_\infty^2)(dP/dx)$, where δ^* is the displacement thickness, U_∞ is the free-stream velocity, ρ is the fluid density and dP/dx is the mean streamwise pressure gradient.

A number of studies have argued that the influence of these additional parameters make APG TBL characteristics inconsistent with popular scaling arguments for canonical wall-bounded flows, such as the classical log-law (Clauser, 1954). Most of these changes can be associated with modifications in the inherent structure of the turbulent flow when exposed to an APG. These modifications are made evident by the wall-normal variation in streamwise normal stress, as represented by the variance of streamwise velocity fluctua-

tions ($\overline{u^2}$) here. In the case of ZPG TBLs, $\overline{u^2}$ profiles have a prominent peak in the inner region of the TBL (referred to as the inner peak), with $\overline{u^2}$ values in the outer region much lower than the inner peak at low-to-moderate Re_τ (Marusic *et al.*, 2015). In contrast, APG TBLs in a similar Re_τ range with moderately strong β , will exhibit a distinct local maximum of $\overline{u^2}$ in the outer region (*i.e.* an outer peak; Monty *et al.*, 2011). Such observations have motivated the proposal of new scaling arguments for the outer region of APG TBLs (Pozuelo *et al.*, 2022). However, the majority of past studies on high Re_τ APG TBLs have unique upstream pressure gradient histories with respect to the measurement locations, owing to the use of ramps in experiments or limited simulation domains with varying β , which are known to influence the magnitude of this outer-peak and its scaling (Bobke *et al.*, 2017).

The primary aim of this study, thus, is to investigate the effect of a moderate APG on the mean streamwise momentum and turbulence structure of a high Re_τ TBL developing from a canonical upstream condition, *i.e.* demonstrating well-established characteristics of a smooth-wall ZPG TBL (Marusic *et al.*, 2015). The proposed investigation will be focused on two parameters: Re_τ and β , which have been investigated individually in past studies but only at low Re_τ (Monty *et al.*, 2011; Pozuelo *et al.*, 2022). Throughout this paper, fluid properties with superscript ‘+’ represent normalization by viscous velocity (U_τ), length (ν/U_τ) and time (ν/U_τ^2) scales. Flow properties in capital, or with overbars, represent mean time-averaged properties, while those in lowercase, represent fluctuations about their respective means. Cartesian coordinates x , y and z represent the streamwise, spanwise and wall-normal directions, respectively, with u , v and w representing the associated velocity components.

EXPERIMENTAL SETUP

Experiments were conducted in the open-circuit, large Melbourne wind tunnel at the University of Melbourne (Marusic *et al.*, 2015; Deshpande *et al.*, 2023). Its test section has a cross-section of $\approx 1.89 \times 0.92 \text{ m}^2$ and a long working section length of 27 m, which permits development of a physically thick turbulent boundary layer ($> 0.3 \text{ m}$) at high Re_τ towards its downstream end. A detailed characterization of the wind tunnel setup for ZPG TBL research can be found in Marusic *et al.* (2015).

In this facility, a ZPG TBL is maintained by installing a high porosity mesh at the test section outlet, which creates

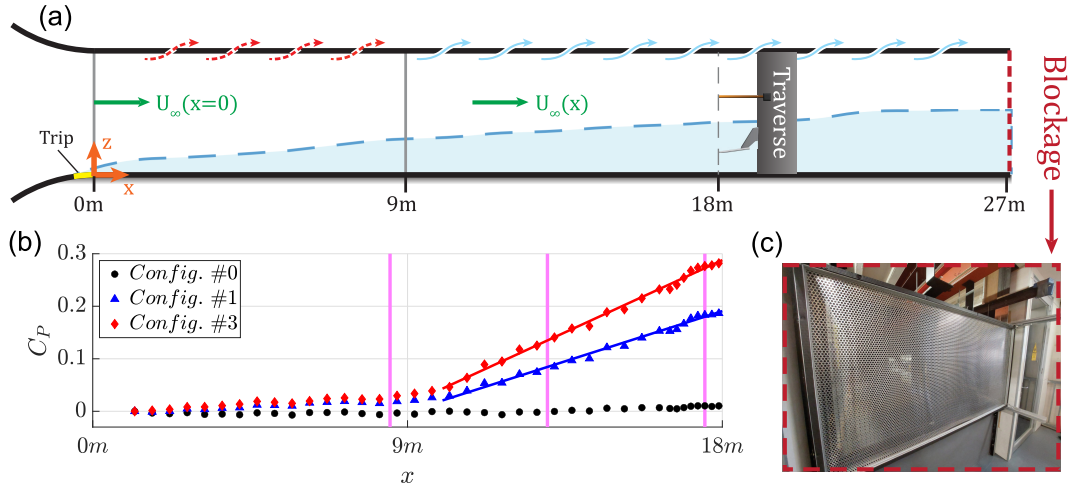


Figure 1. (a) Schematic of wind tunnel experimental setup. (b) Plot of streamwise variation in C_p measured for three screen configurations. Measurement stations indicated by vertical magenta lines (c) Photograph of a single high blockage screen installed at the wind tunnel outlet to increase tunnel static pressure.

| $Config. \#$ | x (m) | Re_τ | β | δ^* (mm) | H_{12} |
|--------------|------------|-----------|---------|--------------------|----------|
| 0 | 8.5 | 4990 | – | 24.1 | 1.31 |
| | 13.0 | 6670 | – | 34.0 | 1.31 |
| | 17.5 | 9030 | – | 44.7 | 1.31 |
| 1 | 8.5 | 4840 | – | 22.8 | 1.30 |
| | 13.0 | 6560 | 0.38 | 37.0 | 1.33 |
| | 17.5 | 7860 | 0.74 | 55.9 | 1.38 |
| 3 | 8.5 | 4590 | – | 21.8 | 1.30 |
| | 13.0 | 6360 | 0.63 | 41.0 | 1.35 |
| | 17.5 | 7590 | 1.45 | 68.1 | 1.43 |

Table 1. Key TBL characteristics.

a nominal back-pressure in the test section. The ceiling of the test section contains an array of air bleed slots, spanning across the tunnel width, which are distributed at regular intervals along the streamwise direction ($\Delta x \sim 1.2 m$; see figure 1a). These air bleed slots allow air to escape in a controlled manner, as a result of the nominal test section back-pressure. The high porosity mesh, in combination with all air bleed slots open, establishes a controlled ZPG across the entire test section fetch (Marusic *et al.*, 2015). This configuration with the high porosity mesh, used for the ZPG TBL, will be referred to as configuration #0, and acts as the baseline for the novel APG experiments (described next).

Figure 1c shows a photograph of an aluminium screen, with a low porosity of 51%. For the APG cases, we install such screens at the outlet of the tunnel test section (downstream of the high porosity mesh described above), to further increase blockage and raise the test section back-pressure. This idea was adapted from the pioneering study of Clauser (1954) which enables development of an APG

TBL with minimum modifications to the test section. In the present study, we fix either 1 or 3 of these low porosity screens (in addition to the original high porosity mesh), to the test section outlet (referred to as configurations # 1 or # 3). This is done to systematically increase the static pressure in the test section. In the upstream part of the test section, however, a nominal ZPG condition is maintained at all times by controlling the outflow from the air bleed slots on the ceiling, up to $x < 9 m$ (see dashed red arrows in figure 1a). This ensures that the APG TBL developing farther downstream always begins from a nominally high Re_τ canonical upstream condition. In the downstream portion of the test section ($x > 9 m$), the air bleed slots remain open such that the increase in back-pressure from the addition of low porosity screens will result in imposition of a moderately strong adverse-pressure gradient condition.

To quantify the pressure gradient conditions, the dynamic pressure, $q = \rho U_\infty^2(x)/2$, was measured at various streamwise locations using a Pitot tube which is attached to

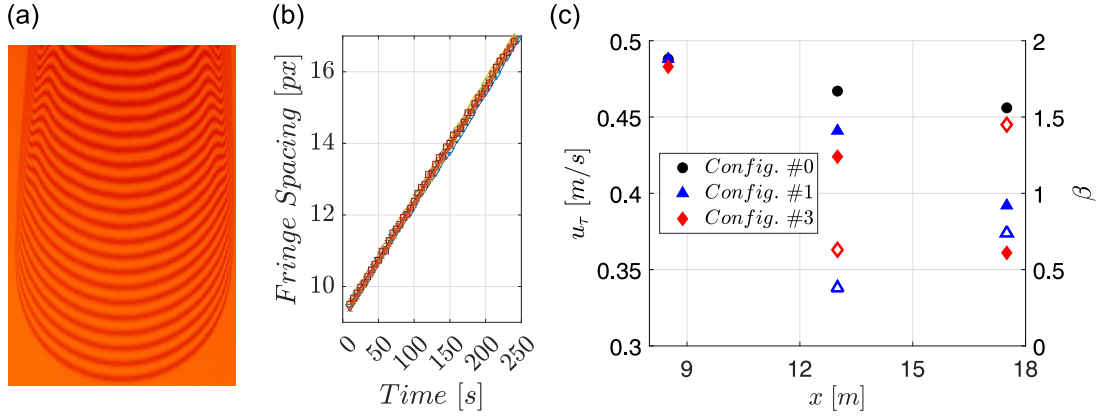


Figure 2. (a) Example photograph of interferogram during a measurement. (b) Example plot of oil-film fringe spacing for the duration of a measurement. (c) Streamwise variation in friction velocity (filled symbols, left vertical axis) measured via OFI, which facilitates estimation of pressure gradient strength β (open symbols; right vertical axis) for each configuration.

the streamwise traverse at a fixed location of $z = 0.525$ m above the wall (figure 1). This wall-normal position guarantees that the Pitot tube is always in the free-stream of both the top- and bottom-wall boundary layers. Atmospheric pressure and temperature were also acquired to compute the free-stream speed from the dynamic pressure measurements. The pressure coefficient along the test section length, $C_P(x)$ is defined as:

$$C_P(x) = 1 - \frac{U_\infty^2(x)}{U_\infty^2(x=0)} \quad (1)$$

The profile of $C_P(x)$ is obtained for each of the three configurations considered (#0, #1 and #3), as shown in figure 1b. We maintained a matched upstream condition of $U_\infty(x=0)/\nu = 9E5$ m⁻¹ for all the measurements reported in this study. The constant and near zero values of C_P , for all three configurations, demonstrates establishment of a nominally ZPG condition for $x < 9$ m, regardless of configuration. This is followed by a quasi linear growth in pressure coefficient ($x > 9$ m) for moderate streamwise APG configurations #1 and #3.

Optical access in the test section wall allowed for OFI measurements to be made at three stations which are marked by the vertical magenta lines in figure 1b. These stations begin in the nominally ZPG upstream region and end at the farthest downstream location within the APG development region. Hot-wire measurements of the TBL were also made possible via the built-in traverse system (figure 1a), which can access all streamwise locations within the test section and precisely control the relative wall-normal movement of the hot-wire sensor. These hot-wire measurements were made at the same stations as the OFI measurements such that the friction velocity obtained through OFI could be applied directly to the hot-wire profiles when normalizing. The key TBL characteristics obtained through the hot-wire and OFI experiments have been documented in table 1 for reference.

OIL-FILM INTERFEROMETRY RESULTS

Friction velocity is an important scaling parameter for wall-bounded flows, and as such, an accurate measurement

of the friction velocity is critical, particularly when investigating non-canonical effects (Marusic *et al.*, 2010). When considering this constraint, OFI emerges as a favourable method by which to measure U_τ in the TBL. And importantly for this study, OFI has previously been used for, and has been shown to be accurate for, high Reynolds number TBLs (Ng *et al.*, 2007).

In principal, the thinning rate of an oil droplet can be measured through thin-film light interference, the pattern of which is directly proportional to the wall shear stress when the effects of gravity and pressure are neglected (Ng *et al.*, 2007). In this experiment, a silicone oil droplet ($\mu_{oil} = 50$ cSt) is placed on a smooth and optically transparent section of the test section wall. As the droplet is spread into a thin film by the wall shear stress over time, it is illuminated by a monochromatic light source which has a slight angle of incidence with respect to the oil film. This creates visible fringe patterns in the oil film which can be captured by a camera, called interferograms, as shown in figure 2a. The rate of change of the spacing between the fringes, as shown in figure 2b, is related to the thinning of the oil film, and thus also relates to the local wall shear stress. In these experiments, a Nikon D800 DSLR camera was used to capture 100 interferograms at 5-second intervals. In each experiment five oil drops were used, spaced evenly in the spanwise direction, which were captured simultaneously in each frame. The results for each individual oil drop could then be ensembled to improve measurement accuracy. The images were processed using a spatial Fourier transform algorithm to extract the fringe spacing from the interferograms. The wall shear stress can then be expressed using the distance between fringes (Δx) over a period of time (Δt) as shown in equation 2 (Fernholz *et al.*, 1996):

$$\tau_w = \mu_{oil} \frac{\Delta x}{\Delta t} \frac{\sqrt{n_{oil}^2 - n_{air}^2 \sin^2 \theta}}{\lambda}, \quad (2)$$

where n_{air} and n_{oil} denote the refractive indices of air and oil, respectively. The parameters θ and λ represent the illumination source incident angle and wavelength, respectively; $\lambda = 589.9$ nm for the monochromatic sodium lamp used in this experiment. The linear development of the fringe spacing over time, shown in figure 2b, demonstrates the quality

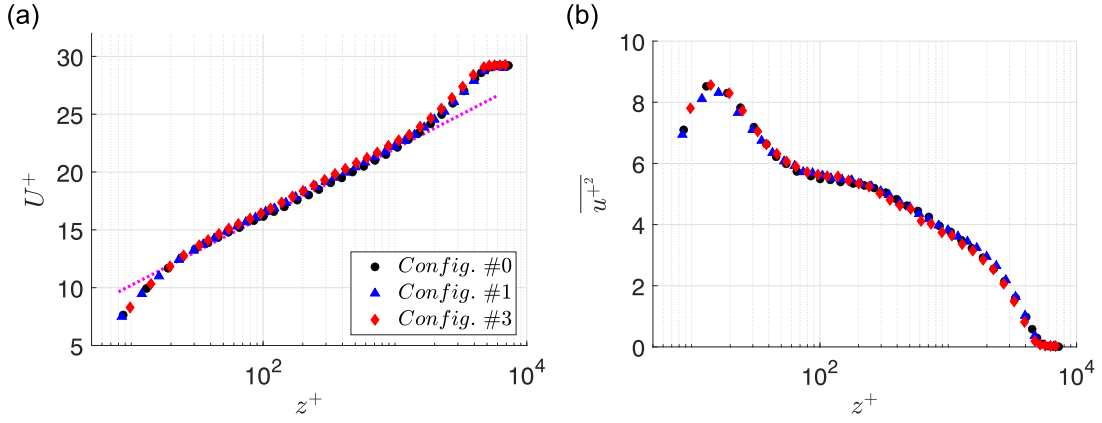


Figure 3. Profiles of (a) mean streamwise velocity and (b) variance of streamwise velocity fluctuations for all configurations measured in the nominally ZPG upstream region ($x = 8.5 m$). Dotted magenta line represents $U^+ = 0.39^{-1} \ln(z^+) + 4.3$.

of the OFI method in the present experiments. The friction velocity can then be determined analytically, from the wall shear stress, as shown in equation 3.

$$U_\tau = \sqrt{\frac{\tau_w}{\rho}} \quad (3)$$

The friction velocities measured using OFI in the present experiments are plotted in figure 2c (filled symbols). At the most upstream location ($x = 8.5 m$), the measured friction velocity does not vary with the configuration of the test section, thereby providing evidence that the flow upstream of $x \lesssim 9 m$ is nominally at a ZPG condition. In each configuration, the friction velocity appears to vary linearly with streamwise distance. For downstream x -locations ($x > 9 m$), the effect of the imposed APG condition can be seen through the decrease in friction velocity as compared to the ZPG case, which is proportional to the APG strength characterized by β . The pressure gradient parameter β is also plotted in figure 2c (open symbols) for reference, the ordinate for which is on the secondary vertical axis (on the right). Considering uncertainties in the OFI method associated with oil viscosity calibration, fringe spacing measurement, and potential contaminants within the oil film, the uncertainty for the friction velocity in this study is estimated to be approximately $\pm 2\%$.

HOT-WIRE RESULTS

In these experiments hot-wire sensors were made in-house from Wollaston wire which was soldered onto Dantec 55P15 boundary layer style probes. The wires were etched with nitric acid to reveal an exposed platinum sensor with a diameter of $d = 2.5 \mu m$ and a nominal length of $l = 0.5 mm$. These dimensions result in an aspect ratio of $l/d = 200$, such that the sensor will not suffer from end conduction effects. Additionally, the spanwise spatial resolution of the sensor for the present experiments will be $l^+ \approx 11 - 16$, resulting in minimal spatial attenuation effects (Hutchins *et al.*, 2009). The hot-wire sampling frequency was set to $f_s = 50 kHz$ and the total sampling time, T_s , was set such that $T_s U_\infty(x) / \delta_{99} > 20000$ for each case to ensure statistical convergence. The chosen sampling frequency results in a temporal resolution of $t^+ = U_\tau^2 / (f_s \nu) = 0.17 - 0.30$, which is again adequate to resolve turbulent scales of interest with

negligible attenuation (Hutchins *et al.*, 2009). All data was low-pass filtered at half of the sampling frequency to avoid high frequency noise and aliasing effects. Calibration of the hot-wire was performed before and after each experiment to account for any drift. The wall-normal hot-wire traverse encoder had a resolution of $\sim 0.1 \mu m$, which ensures accurate estimation of the relative probe displacement in the vertical direction. However, due to wall conduction effects, the first z -location for the hot-wire was limited to $z > 0.2 mm$ above the wall. Fortunately this first z -location was almost always within the viscous sublayer owing to the physically thick turbulent boundary layer being measured here (Deshpande *et al.*, 2023).

Results from these hot-wire measurements are shown in figure 3 and figure 4. We begin by discussing the profiles of the mean streamwise velocity (U^+) and variance of the streamwise velocity fluctuations ($\overline{u'^2}$) measured at the reference upstream location ($x \approx 8.5 m$), which are shown in figures 3a,b. Note, the viscous scaling of all hot-wire profiles presented here, was done using the friction velocity obtained through OFI. Notably, for both statistics, there is a collapse in the profiles from different pressure gradient configurations. The mean velocities also appear to follow the canonical log-law scaling as represented by the dotted magenta line in figure 3a. This confirms that regardless of the pressure gradient condition prescribed in the downstream section, the TBL in the upstream section ($x < 9 m$) remains nominally canonical. The Reynolds numbers and shape factors measured at $x = 8.5 m$, see table 1, additionally demonstrate this fact; the upstream TBL has both a sufficiently high Reynolds number and canonical characteristics, regardless of the configuration. Although not shown here explicitly, these profiles were also found to agree well with previous ZPG TBL studies conducted in the same facility (Hutchins *et al.*, 2009; Marusic *et al.*, 2015; Deshpande *et al.*, 2023).

With the high Re_τ canonical upstream condition confirmed, further development of the TBL under APG conditions can be investigated. In this paper, we will limit our focus to comparing the strongest adverse-pressure gradient configuration, #3, to the zero-pressure gradient configuration, #0. The streamwise profile of the pressure coefficient is plotted again in figure 4a for reference and the pressure gradient strength, β , at each measurement station can be found in table 1 and figure 2c.

The variances in streamwise velocity fluctuations for

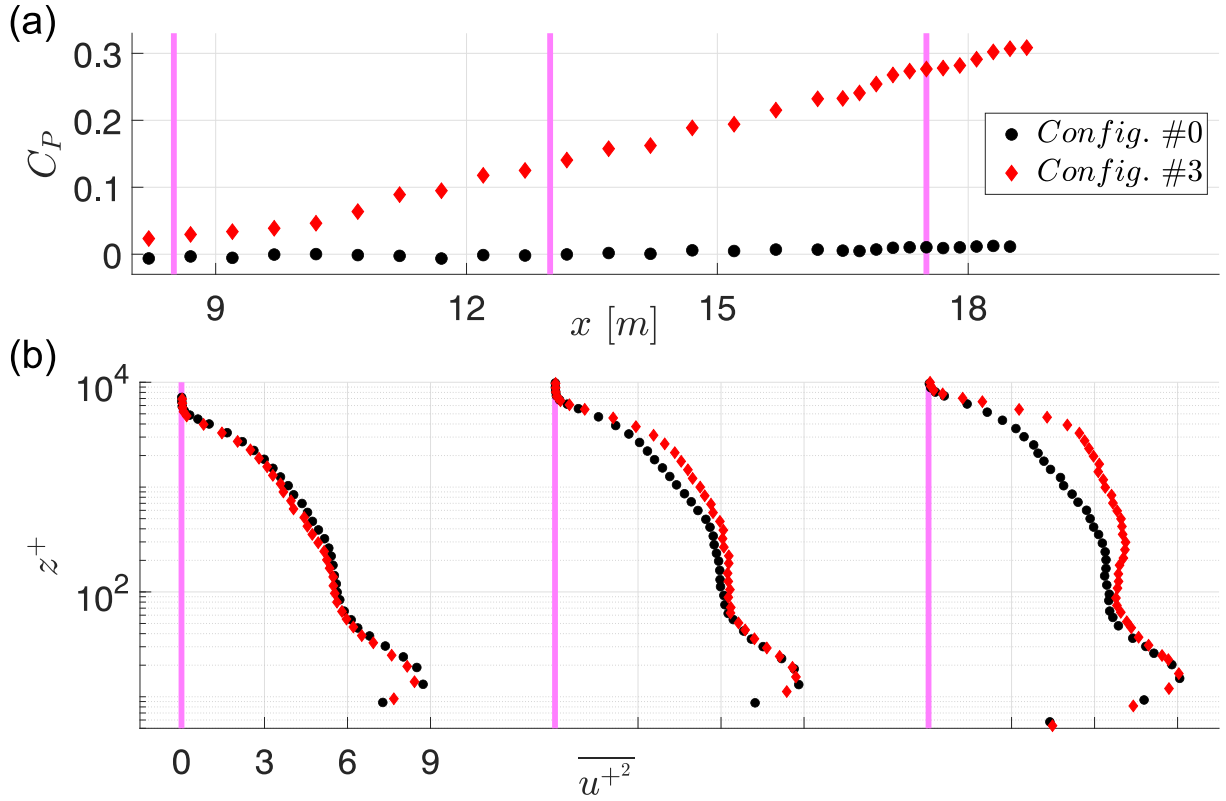


Figure 4. (a) Plot of streamwise variation in C_p for the canonical and strongest adverse pressure gradient configurations. (b) Variance of streamwise velocity fluctuations from three measurement stations as indicated by the vertical magenta lines.

each station and configuration are shown in figure 4b. As expected based on figure 3b, there remains a good agreement between the configurations at $x = 8.5$ m, which establishes the canonical upstream condition. The slight mismatch in the outer region is owing to differences in Re_τ for the two configuration cases. Focusing on the profiles for configuration #0 (i.e. fully ZPG conditions), there is a gradual growth in the variance with downstream evolution, which can be seen as a uniform positive shift in the region between $80 < z^+ < 8000$. This increase is due to the increase in Reynolds number with the downstream location, see table 1 (Marusic *et al.*, 2015). If we now compare between the configurations, i.e. compare between ZPG and APG profiles at the same x -locations, there is a significant increase in the variance for $z^+ > 100$. This is a well-known effect of the adverse-pressure gradient (Pozuelo *et al.*, 2022; Deshpande *et al.*, 2023). This effect is the strongest in the region, around $z^+ = 2000$, which is beyond the log region of the TBL. This leads to the emergence of an outer peak, which can be noted for the farthest downstream location ($x = 17.5$ m), which has the highest β and Re_τ . This, again, is a syndrome of an adverse-pressure gradient (Pozuelo *et al.*, 2022; Deshpande *et al.*, 2023), and cannot be noted in the case of the ZPG TBL.

SUMMARY AND FUTURE WORK

The large Melbourne wind tunnel was modified in order to investigate APG TBLs developing from a ‘canonical’ upstream condition, i.e. developing from a high Reynolds number, smooth-wall, ZPG TBL (Deshpande *et al.*, 2023). These modifications permitted establishment of nominally ZPG conditions in the upstream region ($x < 9$ m), for a range of inlet free-stream velocities, and for a range of adverse-

pressure gradient conditions imposed in the downstream region ($x > 9$ m). OFI and hot-wire measurements were conducted along the long streamwise fetch of the test section, to study the downstream evolution of these unique APG TBLs, with minimal upstream history effects. OFI provided an independent measure of the friction velocity for scaling the hot-wire velocity measurements. Combining these results confirmed that a nominally canonical upstream condition was achieved regardless of the downstream conditions. Typical features of APG TBLs were also demonstrated in the downstream section.

Further measurements and analysis are currently ongoing. From these measurements we will continue to investigate the effect of a moderate APG on the mean streamwise momentum and turbulence structure of high Re_τ smooth-wall TBLs developing under these unique conditions.

REFERENCES

- Bobke, A., Vinuesa, R., Örlü, R. & Schlatter, P. 2017 History effects and near equilibrium in adverse-pressure-gradient turbulent boundary layers. *Journal of Fluid Mechanics* **820**, 667–692, publisher: Cambridge University Press.
- Clauser, F. H. 1954 Turbulent Boundary Layers in Adverse Pressure Gradients. *J. Aeronaut. Sci.* **21** (2), 91–108.
- Deshpande, R., Bogaard, A., Vinuesa, R., Lindić, L. & Marusic, I. 2023 Reynolds-number effects on the outer region of adverse-pressure-gradient turbulent boundary layers. *Physical Review Fluids* **8** (12), 124604.
- Fernholz, N. H., Janke, G., Schober, M., Warner, P. M. & Warnack, D. 1996 New developments and applications of skin-friction measuring techniques. *Measurement Science and Technology* **7**(10):1396.

- Hutchins, N., Nickels, T. B., Marusic, I. & Chong, M. S. 2009 Hot-wire spatial resolution issues in wall-bounded turbulence. *Journal of Fluid Mechanics* **635**, 103–136.
- Marusic, I., Chauhan, K. A., Kulandaivelu, V. & Hutchins, N. 2015 Evolution of zero-pressure-gradient boundary layers from different tripping conditions. *J Fluid Mech.* **783**, 379–411, publisher: Cambridge University Press.
- Marusic, I., McKeon, B. J., Monkewitz, P. A., Nagib, H. M. & Smits, A. J. 2010 Wall-bounded turbulent flows at high reynolds numbers: Recent advances and key issues. *Physics of Fluids* **22(6)**, 1.
- Monty, J.P., Harun, Z. & Marusic, I. 2011 A parametric study of adverse pressure gradient turbulent boundary layers. *Int. J. Heat Fluid Flow* **32** (3), 575–585.
- Ng, H. C., Marusic, I., Monty, J. P., Hutchins, N. & Chong, M. S. 2007 Oil film interferometry in high reynolds number turbulent boundary layers. In *Proceedings of the 16th Australasian Fluid Mechanics Conference*.
- Pozuelo, R., Li, Q., Schlatter, P. & Vinuesa, R. 2022 An adverse-pressure-gradient turbulent boundary layer with nearly constant $\beta \simeq 1.4$ up to $Re_\theta \simeq 8700$. *J. Fluid Mech.* **939**, A34.